

NATURAL HIBISCUS DYE AND SYNTHETIC ORGANIC EOSIN Y DYE SENSITIZED SOLAR CELLS USING TITANIUM DIOXIDE NANOPARTICLES PHOTO ANODE: COMPARATIVE STUDY

SWATI S. KULKARNI^{†,‡,¶}, S. S. HUSSAINI^{§,||}, GAJANAN A. BODKHE^{*,**}
and MAHENDRA D. SHIRSAT^{*,†,††}

**RUSA Centre for Advanced Sensor Technology,
Department of Physics,
Dr. Babasaheb Ambedkar Marathwada University,
Aurangabad 431004, India*

*†Department of Physics,
Dr. Babasaheb Ambedkar Marathwada University,
Aurangabad 431004, India*

*‡Department of Physics, Swa. Sawarkar Mahavidyalaya,
Beed 431122, India*

*§Crystal Growth Laboratory, Department of Physics,
Milliya Arts, Science & Management Science College,
Beed 431122, Maharashtra, India*

*¶meerachothwe@gmail.com
||shuakionline@yahoo.co.in
**gabodkhe@gmail.com
††mdshirsat.phy@bamu.ac.in*

Received 5 December 2017
Revised 2 January 2018
Accepted 24 January 2018
Published 15 March 2018

Titanium dioxide (TiO₂) nanoparticles have been synthesized by the cost effective Sol–Gel technique. Characteristics of TiO₂ nanoparticles were investigated by X-ray diffraction and Fourier Transform Infrared spectroscopy. The Eosin Y dye and dye extracted from Hibiscus tea have been successfully used in fabrication of the dye sensitized solar cell. The photovoltaic performance of the dye sensitized solar cell indicates that the short circuit photo current, open circuit voltage and efficiency of the DSSC using Eosin Y dye is 10 times more compared to the DSSC using the Hibiscus dye.

Keywords: Titanium dioxide nanoparticles, Eosin Y dye, hibiscus dye, dye sensitized solar cell (DSSC).

1. Introduction

Solar Cell is a clean, environmental friendly source of electricity converting light energy into electrical

energy. As the Dye Sensitized Solar Cells (DSSCs) are using non-toxic materials and requiring little energy to manufacture, they are generally considered much

††Corresponding author.

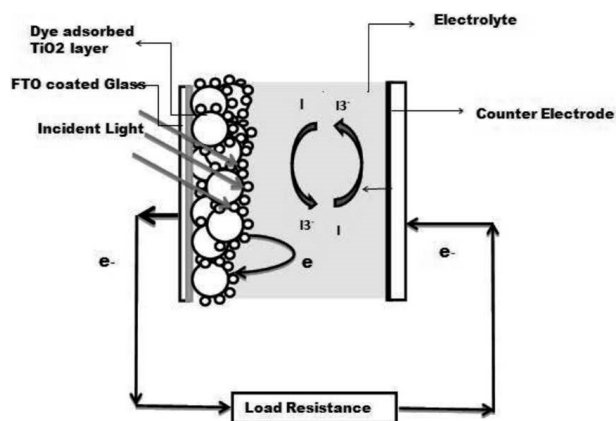


Fig. 1. Working principle of DSSC.

more environmentally affable than the conventional silicon-based solar cells.^{1,2} In the DSSCs, electrons from the valence band of excited dye are injected into the conduction band of the semiconductor oxide, followed by dye regeneration with the help of electrolyte and moving hole to the counter electrode,³⁻⁵ as shown in (Fig. 1). Extensive large amount of work has been done on dye molecules,^{6,7} semiconductor TiO₂ electrodes,⁸⁻¹⁰ counter electrodes¹¹⁻¹³ and electrolytes¹³⁻¹⁵ to improve the DSSC efficiency and stability. The performance of the DSSC is mainly dependent on the dye used as a sensitizer in addition to many other parameters like the photo electrode materials, the redox couple chosen and the back electrode materials. The absorption spectrum of the dye and its linkage to the surface of semiconductor oxide is the most important parameter in determining the efficiency of the DSSC.¹⁶

Till date, ruthenium bipyridyl dye compounds are the most successful dyes for DSSC. This has been characterized as a large absorption coefficient in the visible part of the solar spectrum. Good absorption, excellent stability and efficient electron injection are the merits of ruthenium dye¹⁷⁻²¹; however, the main issues are its cost and complicated purification steps. Moreover, it is toxic and carcinogenic and containing metals, hence hazardous.⁶ Therefore, there is an intense need to study the natural metal free dyes as sensitizers in DSSC. Many natural organic dyes have been studied extensively and tested as low cost alternatives to replace rare, expensive and environmentally hazardous ruthenium dyes.²²⁻²⁵ Commonly studied natural dyes include tannins, chlorophyll,²⁶ flavonoids,²⁷ xanthene²⁸ and anthocyanin.²⁹ Eosin Y dye is one of the best xanthene

dyes³⁰ and Hibiscus is the commonly used anthocyanins.³¹ Though the efficiency of DSSC using natural dye or organic dye is far away from commercialization, these have been studied because of their environmental friendliness, non-toxicity, abundant availability, cost efficiency and easy and robust processing.³² In the present study, investigation of a xanthene derivative of natural dye i.e. Eosin Y dye and natural hibiscus tea dye as a photo sensitizer has been done.

2. Material and Method

2.1. Materials

Titanium iso-propoxide (TTIP from Otto chemicals Germany), and anhydrous ethanol (EtOH) were used for preparing TiO₂-Sol. Polyethylene glycol was purchased from Otto Chemicals India, Eosin Y Dye and Chloroplatinic acid (H₂PtCl₆) were purchased from Ward Hill, U.S.A. Anhydrous Lithium iodide and iodine along with acetonitrile were used as redox couple. All chemicals received were used as it is without further purification.

2.2. Preparation of pure TiO₂ nanoparticles

TTIP:EtOH:H₂O:HCl were taken in the proportion of 1:15:60:0.2 and were used to prepare TiO₂-Sol. Ethanol and hydrochloric acid (HCl) was added to deionize (DI) water to have the pH nearly two. TTIP solution was dropped into the above mixture solution with vigorous stirring and stirring was continued for 48 h and then it was allowed to edge, filtered, washed several times using DI water and ethanol and then dried at 80°C until the brownish crystals were obtained. The crystals were ground and sintered for one hour at a temperature of 450°C to obtain white powder of TiO₂ nanoparticles.

2.3. DSSC fabrication

For studying the performance of the hibiscus and Eosin Y dyes as photosensitizers on TiO₂ thin film electrode, the sandwich type cells were fabricated. Cleaned Florin-doped SnO₂ glass plates of dimension 2 × 2 cm were used for anode and cathode preparation. Anode and cathode area was decided to be 1 sq. cm. The anodes were prepared by the doctor blade method,

and the cathodes were formed by the drop-casting the Chloroplatinic acid solution in the 2-propanol. Both anode and cathode were dried on the hot plate for 10 min and sintered for an hour at 450°C.

To assemble the cell, the cathode was put over the anode with scotch tape spacer and bound together with the crocodile clips. An electrolyte solution composed of 0.5 M LiI and 0.05 M Iodine in Acetonitril was introduced into the cell by capillary action.

Phase of the TiO₂ nanoparticles was determined using BRUKER-binary V3 X-ray diffraction (XRD) spectrophotometer. Absorption spectra of TiO₂ nanoparticles and dyes were investigated with Shimadzu 1800 UV visible spectrophotometer. FTIR fingerprints of TiO₂ nanoparticles were inspected using Brooker IR spectrophotometer.

V-I characteristics of DSSCs were studied using Keithley 2400 source meter along with 250W halogen lamp of the overhead projector. Assembly for *I-V* characteristics was calibrated using a standard Silicon solar panel to obtain the irradiance of 100 mW/cm² under direct sunlight.

3. Results and Discussion

3.1. Crystallographic study of TiO₂ nanoparticles

Figure 2 shows the XRD pattern of TiO₂ nanoparticles prepared by sol-gel route. The highest intensity of (101) peak at 2θ equal to 25°C indicates the

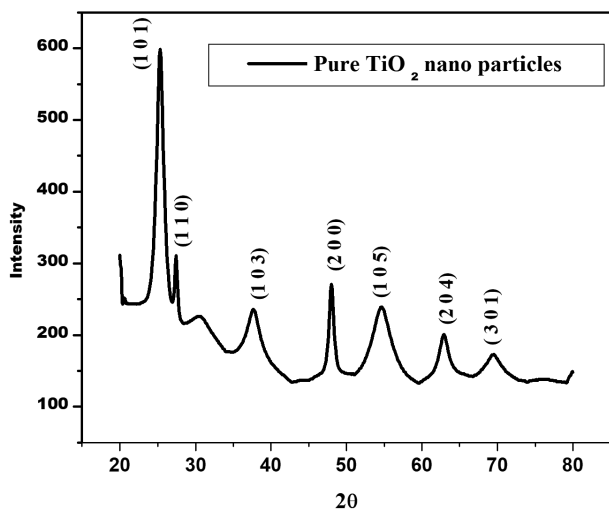


Fig. 2. XRD pattern of TiO₂ nanoparticles synthesized by Sol-Gel route.

Table 1. XRD peaks at different 2θ values, their corresponding plane/phase of the TiO₂ nanoparticles.

No.	Position [2θ]	Peak plane/phase
1	25.3092	101/A
2	27.4212	110/R
3	37.6909	103/A
4	48.0116	200/A
5	54.6474	105/A
6	62.9161	204/A
7	69.4778	301/R

formation of anatase phase TiO₂ nanoparticles. The other peaks and their corresponding planes are tabulated in Table 1. All these peaks in the XRD pattern were indexed by comparing with the JCPDS file numbered 21-1272 and 21-1276.^{19,33} A small peak at 27.4 corresponds (110) plane and indicates the presence of the rutile phase nanoparticles in small proportion.^{33,34} However, the proportion of anatase phase, calculated using Eq. (1) was found to be 67.83%.

$$\text{weight fraction Anatase} = \frac{100}{1 + 1.265 * \left(\frac{I_R}{I_A}\right)}, \quad (1)$$

where IA and IR are intensities of anatase (101) and rutile (110) diffraction, respectively.³³

The full width at half maxima for intense (101) peak corresponding to anatase phase was obtained using Xpert high score software and used to calculate the size of nanoparticles using the Scherrer formula given by Eq. (2)

$$\text{Size of nanoparticle } D = \frac{K\lambda}{\beta \cos \theta}, \quad (2)$$

where *K* is the shape factor having value 0.89, *λ* is the wavelength of incident CuKα radiations having value 1.54 nm and *β* is the Full width at half maxima.

The size of nanoparticles was obtained to be 12.28 nm using Eq. (2).

3.2. FTIR analysis

Formation of TiO₂ nanoparticles was confirmed by FTIR spectrograph (Fig. 3). Usually, the characteristic vibrations of the inorganic Ti–O stretching vibrations are observed in the range 400 to 900 cm⁻¹. A sharp peak at 742 cm⁻¹ indicates the bond formation due to the bending vibrations of Ti–O–Ti whereas

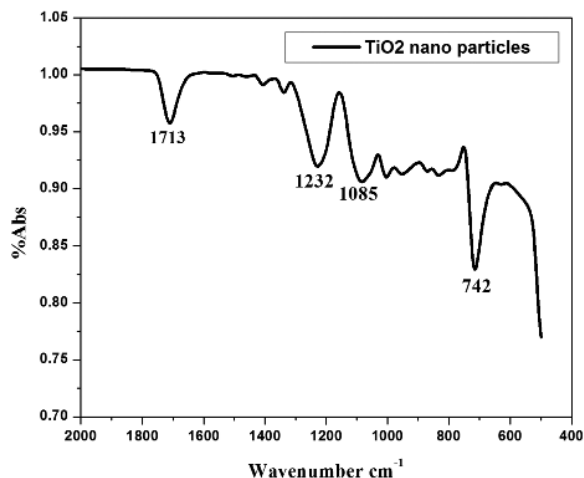


Fig. 3. FTIR spectrograph of TiO₂ nanoparticles.

the peak at 1232 cm⁻¹ is indicating stretching vibrations of the Ti–O–Ti. Peak at 1713 cm⁻¹ is attributed to the bending vibrations of the OH group. There was no peak observed after 1713 cm⁻¹ which means that all the organic compounds were removed from the samples after calcination.

3.3. Absorption spectra of Eosin Y and Hibiscus extracts

The UV–visible spectral study of the Eosin Y and hibiscus tea extraction dye was carried out using 2450 spectrophotometer in the wavelength range 300 nm to 900 nm. Figures 4(a) and 4(b) show absorption

spectra of Eosin Y and Hibiscus tea extracts dyes, respectively. It was observed from the spectra that there was broad absorption peak at 511 nm for Eosin Y dye whereas for Hibiscus tea extract dye, the absorption peak was observed at 379 nm and it was quite sharp. The band gap of both the dyes was calculated using Eq. (3).³⁵

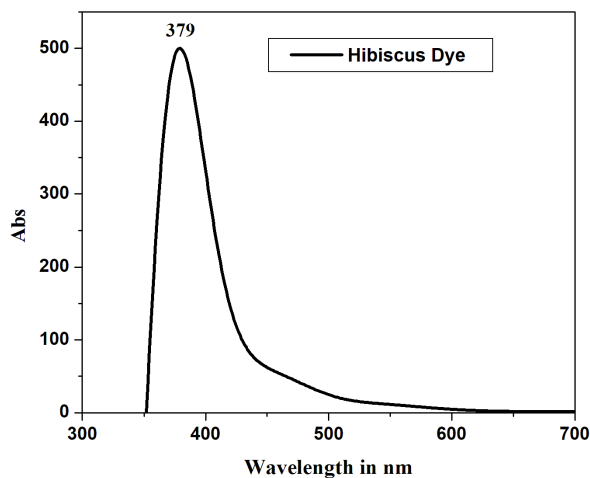
$$E_g = \frac{hc}{\lambda e} \text{ eV}, \quad (3)$$

where h is Planck's constant having value 6.63×10^{-34} Jsec, C is the velocity of light having value 3×10^8 m/sec, λ is the peak absorption Wavelength, e is the charge on electron.

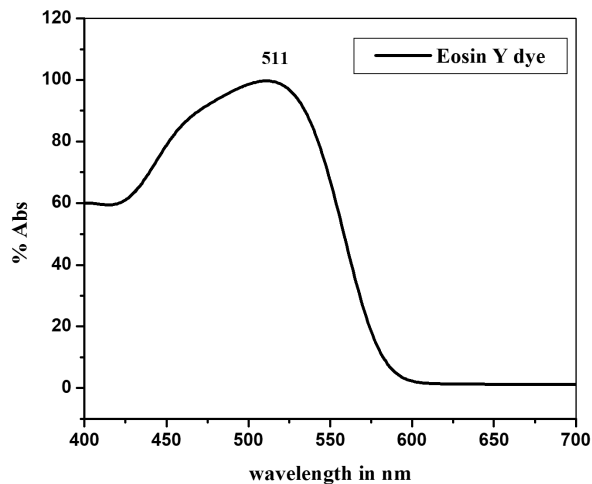
Using Eq. (3), the band gap calculated for Eosin Y dye was 2.43 eV and for Hibiscus dye it was 3.28 eV. As the absorption peak for Eosin Y dye was broader, the photons having energy 2.29 eV to 2.75 eV had chances to be absorbed and produce photoelectrons. Whereas the absorption peak for hibiscus dye being sharp the photoelectrons having energy greater than 3.28 eV can cause the photoexcitation of dye molecules.

3.4. Photovoltaic characteristics of DSSCs

The performance of Hibiscus tea extract and Eosin Y dye as sensitizer has been evaluated by determining short circuit current (I_{sc}), open-circuit voltage (V_{oc}), Fill Factor (FF) and energy conversion efficiency (η)



(a)



(b)

Fig. 4. (a) UV–visible spectra of Eosin Y Dye, (b) UV–visible spectra of hibiscus dye.

Table 2. Photovoltaic parameters — maximum current, maximum voltage, Short circuit current, open circuit voltage, fill factor, efficiency using Eosin Y and Hibiscus dye.

Sensitizer	I_m	V_m	I_{sc}	V_{oc}	FF	%Eff
Eosin Y	$10.2 \mu\text{A}$	32 mV	$21.9 \mu\text{A}$	62.8 mV	0.24	3.28×10^{-4}
Hibiscus	$0.446 \mu\text{A}$	26 mV	$0.917 \mu\text{A}$	46.7 mV	0.27	4.6×10^{-5}

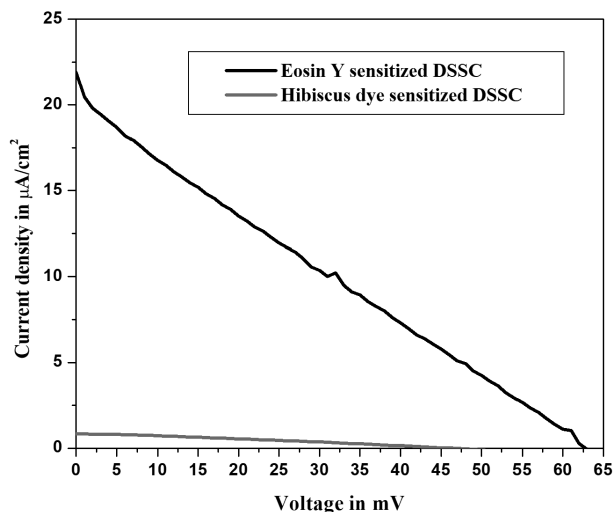


Fig. 5. Current density — Voltage performance of DSSC sensitized by Hibiscus dye and Eosin Y dye.

under the irradiance of $100 \text{ mW}/\text{cm}^2$. The typical I-V curves of a DSSC have been shown in Fig. 5 and the device performance parameters derived from J - V -curves are listed in Table 2. From Table 2, it could be revealed that V_{oc} , I_{sc} , η for DSSC using Eosin Y dye is comparatively better than DSSC using hibiscus tea extract dye. Less efficiency for both dye sensitized solar cells may be attributed to the robust nature of dye extraction and adsorption. Efficiency of DSSC using Eosin Y dye was observed to be 10 times more as compared to the efficiency of DSSC using hibiscus extracted dye.

4. Conclusion

The Photovoltaic performance of the Hibiscus tea dye and Eosin Y dye has been investigated by employing them as photosensitizer in the porous TiO_2 nanoparticles-based Solar Cell. Eosin Y dye sensitized solar cell exhibits better performance as compared to Hibiscus dye sensitized solar cell. Simple preparation method, wide availability, low cost and environmental

friendliness of these dyes make them attractive for their use as sensitizers in dye sensitized solar cells.

Acknowledgment

Authors are grateful to UGC-SAP, New Delhi, India (F.530/16/DRS-I/2016 (SAP-II)), Director, RUSA Centre for Advanced Sensor Technology, Dr. Babasaheb Ambedkar Marathwada University, Aurangabad, India for providing technical support.

References

1. G. Calogero *et al.*, *Chem. Soc. Rev.* **44** (2015) 3244.
2. P. Hecht, Humboldt University of Berlin (2012). Available at <http://edoc.hu-berlin.de/dissertationen/menting-raoul-2012-11-16/PDF/menting.pdf>.
3. G. P. Smestad and M. Gratzel, *J. Chem. Edu.* **75** (1998) 752.
4. M. Grätzel, *J. Photochem. Photobiol. C* **4** (2003) 145.
5. C. Cavallo *et al.*, *J. Nanomater.* **1** (2017) 31. <http://doi.org/10.1155/2017/5323164>.
6. H. S. El-Ghamri *et al.*, *J. Nano-Electron. Phys.* **7** (2015) 03001.
7. Z. A. Shah *et al.*, *J. Fundamental Renew. Energy Appl.* **7** (2017) 234. doi: 10.4172/20904541.1000234.
8. C.-Y. Huang *et al.*, *Sol. Energy Mater. Sol. Cells* **90** (2006) 2391.
9. T. T. Nguyen *et al.*, *Mater. Chem. Phys.* **144** (2014) 114.
10. M. Rokhmat *et al.*, *Proc. Eng.* **170** (2017) 72.
11. S. Thomas *et al.*, *J. Mater. Chem. A* **2** (2013) 4474, doi: 10.1039/C3TA13374E.
12. X. Guo *et al.*, *Front. Energy Res.* **3** (2015) 50, doi: 10.3389/fenrg.2015.00050.
13. M. Chen and L.-L. Shao, *Chem. Eng. J.* (2016), doi: <http://dx.doi.org/10.1016/j.cej.2016.07.001>.
14. K. T. H. Ze Yu, *Chemical Science and Engineering*, Royal Institute of Technology SE-100 44 Stockholm, Sweden (2012).
15. Z. S. Wang *et al.*, *J. Phys. Chem. B* **109** (2005) 22449, doi: 10.1021/jp053260h.
16. G. S. Selopal *et al.*, *Scientific Reports* **6** (2016) 18756, doi: 10.1038/srep18756 1.
17. W. A. Ayalew, D. W. Ayele, *J. Sci.* **1** (2016) 488.
18. V. Sugathan *et al.*, *Renewable and Sustainable Energy Reviews* **52** (2015) 54.

19. R. Govindaraj et al., *Int. J. Chem. Tech. Res.* **6** (2014) 5220.
20. S. S. Mali et al., *Electrochimica Acta* **59** (2012) 113.
21. K. Shahu and V. V. S. Murti, *Indian Journal of Pure and Applied Physics* **154** (2016) 485.
22. M. A. M. Al-Alwani et al., *Int. J. Electrochem. Sci.* **12** (2017) 747.
23. M. Hosseinnzhad et al., *Curr. Sci.* **109** (2015) 956.
24. N. Yazie et al., *Mater. Renew. Sustain. Energy* **5** (2016) 13.
25. L. Amadi et al., *Nanosci. Nanoeng.* **3** (2015) 25.
26. R. Syafinar et al., *Energy Procedia* **79** (2015) 896.
27. M. R. Narayan, *Renewable and Sustainable Energy Reviews* **16** (2012) 208.
28. Kark et al., *NJST* **13** (2013) 179.
29. J. O. Ozuomba et al., *Adv. Appl. Sci. Res.* **4** (2013) 60.
30. Y. Zhou et al., *Chin. Sci. Bull.* **54** (2009) 2633. <https://doi.org/10.1007/s11434-009-0440-8>.
31. R. F. Mansa et al., *J. Phys. Sci.* **25** (2014) 85–96.
32. K. Kakiage et al., *Scientific Reports* **6** (2016) 35888, doi: 10.1038/srep35888.
33. M. M. Ba-Abbad et al., *Int. J. Electrochem. Sci.* **7** (2012) 4971.
34. Z. Liu et al., *Asian J. Chem.* **26** (2014) 655.
35. P. Das et al., *Phys. Chem. Chem. Phys.* **18** (2016) 1429, doi: 10.1039/C5CP04716A.